

# A new class of coupled continuum equations for atomic growth on surfaces

Biplab Sanyal<sup>†</sup>, Anita Mehta<sup>‡</sup>|| and Abhijit Mookerjee<sup>†</sup>

<sup>†</sup> S N Bose National Centre for Basic Sciences, JD-Block, Sector-III, Salt Lake, Calcutta 700091, India

<sup>‡</sup> Clarendon Laboratory, Parks Road, Oxford OX1 3PU, UK

E-mail: [biplab@boson.bose.res.in](mailto:biplab@boson.bose.res.in), [anita@boson.bose.res.in](mailto:anita@boson.bose.res.in) and [abhijit@boson.bose.res.in](mailto:abhijit@boson.bose.res.in)

Received 4 December 1998, in final form 23 April 1999

**Abstract.** We propose a new class of coupled equations for describing interfacial growth by molecular beam epitaxy and, additionally, present some *ab initio* electronic structure calculations for energetics in support of our equations. Finally, we present our results for the critical spatial ( $\alpha$ ) and temporal ( $\beta$ ) roughening exponents for our model and analyse our results in the context of atomic interfaces.

## 1. Introduction

The study of kinetic growth equations [1] and their relevance to real experimental deposition techniques has become a challenging and fascinating topic. Such deposition processes are particularly important for the understanding of physical properties of the resulting surfaces. This is vital for technological reasons. In this communication we modify a class of coupled stochastic differential equations suggested earlier by Mehta *et al* [2, 3] for driven sandpiles, and study them as models for surface epitaxial growth of metals on metallic substrates.

While non-equilibrium growth has been extensively studied by means of coarse-grained classical stochastic equations (see [1]), it is not obvious *a priori* that the microscopic constraints relevant to atomic surfaces would automatically be satisfied by largely heuristic classical terms. In this communication we therefore present electronic energy calculations in support of our model.

The plan of this paper is as follows:

- (i) First, we shall adopt ideas introduced earlier in the field of granular media and modify them to model atomistic deposition processes. We shall therefore qualitatively justify each term in our deposition equations.
- (ii) Second, we shall numerically solve the equations for model situations to study the morphology of the rough surfaces which result from them. We shall vary parameters in our model equations to see their effect on the resulting surfaces and observe whether the results tally with the qualitative ideas put forward earlier.

|| On leave from: S N Bose National Centre for Basic Sciences, Calcutta, India.

- (iii) Finally, we shall carry out first-principles electronic structure calculations on a specific example: deposition of bcc Fe on the (100) surface of fcc Ag, using the tight-binding linearized muffin-tin orbitals recursion (TB-LMTO recursion) and the orbital peeling method to study the local chemical potentials on a rough surface produced by the deposition equations, and attempt to justify some of the basic assumptions behind the model.

In the so-called *first-principles* molecular dynamics [4] in vogue these days, the motion of the constituent atoms or groups of atoms is usually considered to be classical. Quantum mechanics plays the pivotal role in determining the force between them; in a metal, this force is provided by the valence electron cloud. Our approach in the following calculations will be similar. *The actual growth of the atomic surface will be determined classically*, via the solution of the coupled continuum equations that we will present; on the other hand, *the chemical potential will be generated by quantum electronic energy calculations*.

## 2. The non-linear coupled continuum equations

Among various physical processes which have been taken into account in models of growing interfaces, *surface diffusion* has been considered as the most important process involved in surface growth. One such equation is the linear fourth-order Mullins–Herring continuum equation [5] supported by the discrete model of Wolf and Villain (WV) [6]:

$$\partial h(\mathbf{x}, t)/\partial t = -D_h \nabla^4 h(\mathbf{x}, t) + \eta(\mathbf{x}, t) \quad (1)$$

where  $h(\mathbf{x}, t)$  is the height of the interface measured from some mean height  $\langle h(\mathbf{x}, t) \rangle$  and  $\eta(\mathbf{x}, t)$  represents Gaussian white noise as usual. This equation yields a large roughness exponent  $\alpha = 1.5$  for  $d = 1$ , where  $d$  is the dimension of the substrate.

Although there have been a number of non-linear equations which add to this simple linear description [7] of epitaxial surface growth, there have been rather few attempts so far that look separately at the roles of relatively immobile atoms which are bonded to the surface (forming clusters) and the cloud of mobile atoms above the surface. The latter arise both from the impinging atomic beam and from evaporation caused by atoms knocked out of the surface by thermal or mechanical disturbances. These are described by their local density  $\rho(\mathbf{x}, t)$ . We propose a new class of growth equations with an explicit coupling between the profile of ‘bonded’ atoms represented by the local height of the surface  $h(\mathbf{x}, t)$ , and ‘mobile’ atoms on the surface represented by their local density  $\rho(\mathbf{x}, t)$ . Our equations read

$$\partial h/\partial t = -D_h \nabla^4 h - \mathcal{T} + \eta_h(\mathbf{x}, t) \quad (2)$$

$$\partial \rho/\partial t = D_\rho \nabla^2 \rho + \mathcal{T} \quad (3)$$

where the transfer term  $\mathcal{T}$  is given by

$$\mathcal{T} = (v - \rho)|\nabla h|. \quad (4)$$

Earlier work of Barabasi [8] also made use of the formalism of coupled equations; this however, merely made use of gradient expansions of the sort that have been familiar since the work of Kardar *et al* [9]. Where our work hits novel ground is in its introduction of coupling terms from a phenomenological viewpoint, as a result of which its consequences are rather more physical. In particular, even at the formal level, Barabasi was unable to obtain a crossover to another universality class, keeping to what he termed the superdiffusive regime, whereas in all of our work, interesting crossovers have been observed.

We describe in what follows the meaning of the above terms. In items (i) and (ii), we describe those terms which are specific to a single species, whereas in items (iii) and (iv) we describe the coupling terms included in the transfer term  $\mathcal{T}$ .

- (i) The fourth-order term in equation (2) describes surface diffusion of bonded atoms; this is the usual WV [6] term where  $D_h$  represents a diffusivity. The particle current leading to this term is the gradient of the local chemical potential, which is assumed to be proportional to the local curvature.
- (ii) The unattached, flowing atoms are neither bonded to one another nor to atoms on the surface. The first term in equation (3) hence describes normal, as opposed to surface, diffusion of the mobile atoms, where the corresponding current is the gradient of the density.
- (iii) The first term in the transfer term  $\mathcal{T}$ , equation (4), describes spontaneous generation of mobile atoms on the surface or *evaporation*. This could be due to ‘vibration’ caused by, for example, thermal disturbances. We have assumed that it is easier thermally to eject atoms bonded at high slopes on the clusters.  $\nu$  then is a measure of the substrate temperature.
- (iv) The second term in  $\mathcal{T}$ , equation (4), represents *condensation*, whereby mobile atoms accumulate and accrete preferentially at points of high slope.
- (v) Finally the last term in equation (2) is a Gaussian white noise characterized by its width  $\Delta_h$ :

$$\langle \eta_h(\mathbf{x}, t) \eta_h(\mathbf{x}', t') \rangle = \Delta_h^2 \delta(\mathbf{x} - \mathbf{x}') \delta(t - t').$$

We assume that growth occurs on a flat substrate; this and the absence of a preferred direction causes us to consider always the absolute values of the slope in the above equations. We emphasize that our modelling in the above equations represents the well-known physics of molecular beam epitaxially (MBE) grown surfaces via *surface diffusion* of interfacially bonded atoms, *ordinary diffusion* of mobile atoms above the interface, and the interconversion of one species into the other via *evaporation* and *condensation* [11].

We can visualize the following sequence of processes: first, the mobile atoms diffuse ( $\nabla^2 \rho$ ) in the cloud above the surface. This is followed by the preferential conversion of these atoms into the bonded species at points of high slope ( $\rho |\nabla h|$ ) on the surface such as mounds and grooves. The term  $\nu |\nabla h|$  models the effect of evaporation, leading to a dynamical exchange at regions of high slope between bonded and unbonded atoms.

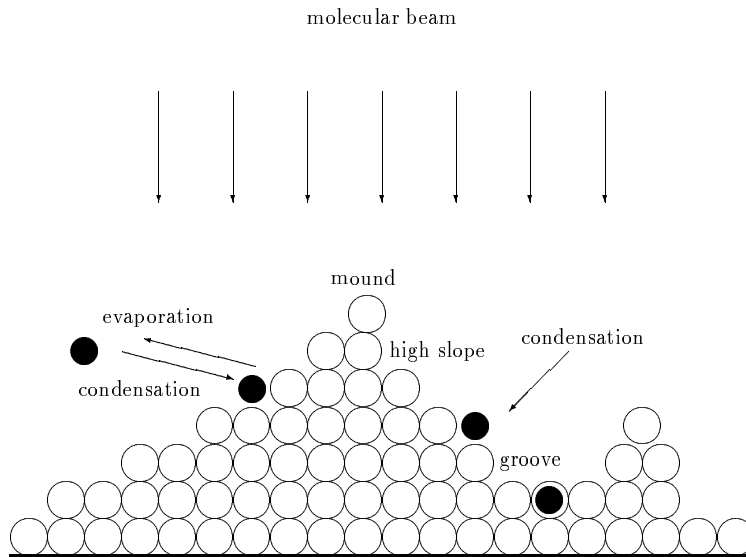


**Figure 1.** A schematic diagram of various features of our model

However, the action of the  $\nabla^4 h$  term is to stabilize the formation of mounds and grooves, so ultimately the overwhelming effect is a roughening of the surface. Figure 1 illustrates the effect of the terms in our model.

### 3. A model example and its rough surfaces

We have simulated the above equations in  $d = d' + 1$  dimensions, with  $d' = 1$  where  $d'$  is the substrate dimension, in order to study the morphology of the resulting rough surfaces. We have chosen scales such that the diffusion constants  $D_h$  and  $D_\rho$  are taken to be 1. The noise amplitude  $\Delta_h$  is taken to be  $10^{-3}$ . We have varied the parameter  $\nu$  between  $10^{-6}$  and 0.01.

In figure 2 we have shown a portion of the rough surface layer produced at different time steps. On the left, the surfaces are shown to scale. We note that the surface width increases with time. The panel on the right shows the same surfaces scaled down to  $-1 \leq h \leq 1$  in order to bring out the detailed features. We note that with increasing time steps, the short-length-scale features slowly disappear, and mounds and grooves spanning larger lengths are formed.

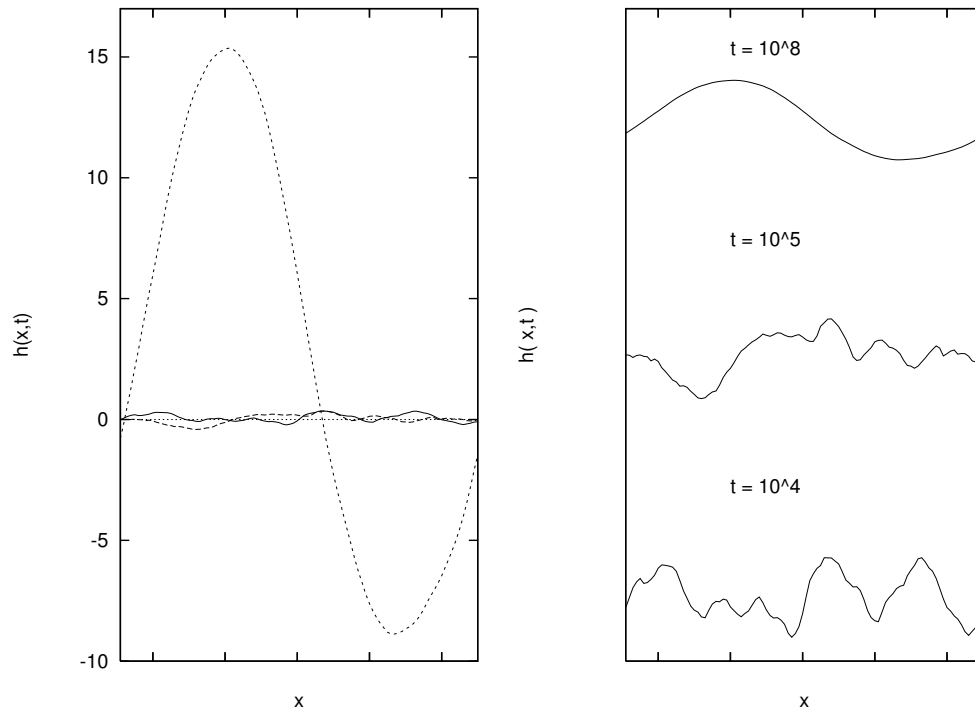


**Figure 2.** A part of the rough surface produced at different times  $t = 10^4$ ,  $10^5$  and  $10^8$  time steps: (left) shown to scale, and (right) scaled to  $-1 \leq h \leq 1$  to bring out the details. Here  $\nu$  is taken as 0.01 and  $x$  is scaled to the range  $0 \leq x \leq 1$ .

Figure 3 shows a similar profile for the density  $\rho$ . Very similar statements may be made about these profiles. It is interesting to compare the profiles of  $h$  and  $\rho$  at large times. In the  $h$ -profile, the local curvature is concave with respect to the substrate near the tops of the mounds, implying that the local coordination of bonded atoms is small. Moreover the local slopes here are also large. Atoms in these regions are very loosely bonded and, according to our model, are the ones which most easily evaporate. In these regions we expect the local density

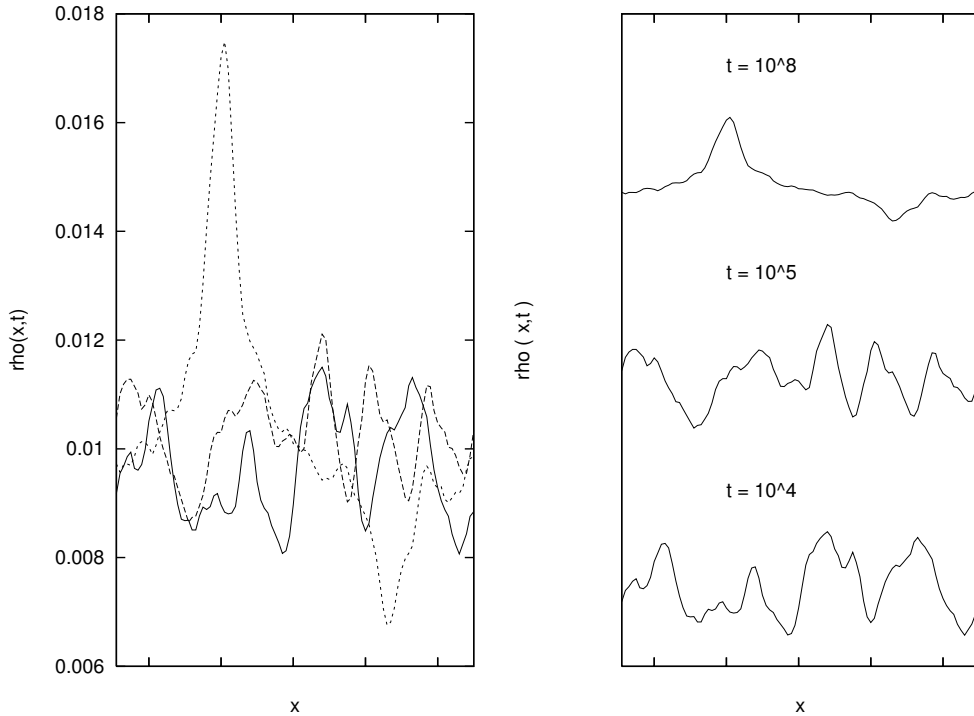


**Figure 3.** A part of the rough density profile produced at different times  $t = 10^4, 10^5$  and  $10^8$  time steps: (left) shown to scale, and (right) scaled to  $-1 \leq \rho \leq 1$  to bring out the details. Here  $\nu$  is taken as 0.01 and  $x$  is scaled to the range  $0 \leq x \leq 1$ .

of mobile atoms (formed from evaporation) to be large. This is indeed seen in the density profile of  $\rho$ . Similarly, within grooves, where the local curvature is convex with respect to the substrate and the local coordination of bonded atoms is large, it is more difficult to knock off atoms by evaporation. Here we expect the local density of mobile atoms to be smaller, which is indeed what we observe. In our model, there should thus be a positive *local* correlation between the height and density profiles.

This correlation can be measured by the standard correlation coefficient defined as

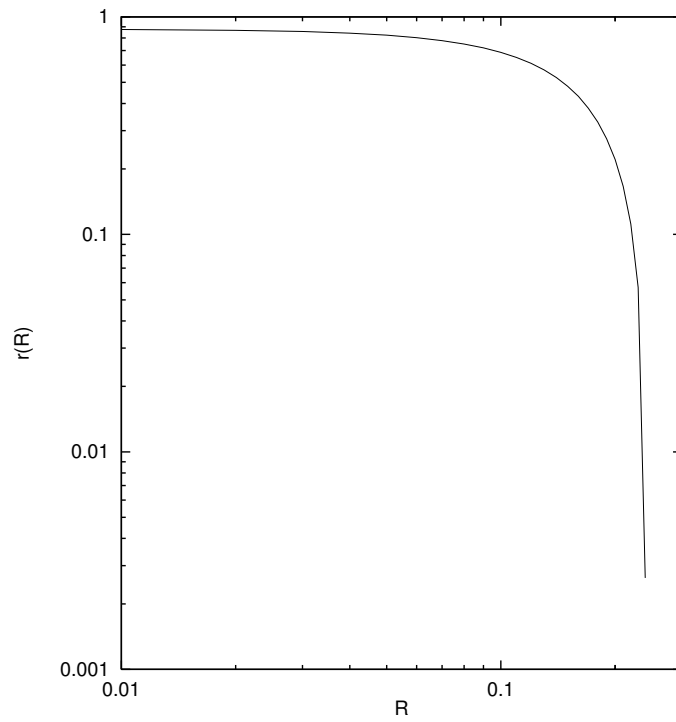
$$r(R) = \frac{\text{cov}(h(r, t), \rho(r + R, t))}{[\text{var}(h(r, t)) \text{var}(\rho(r + R, t))]^{1/2}}$$

where

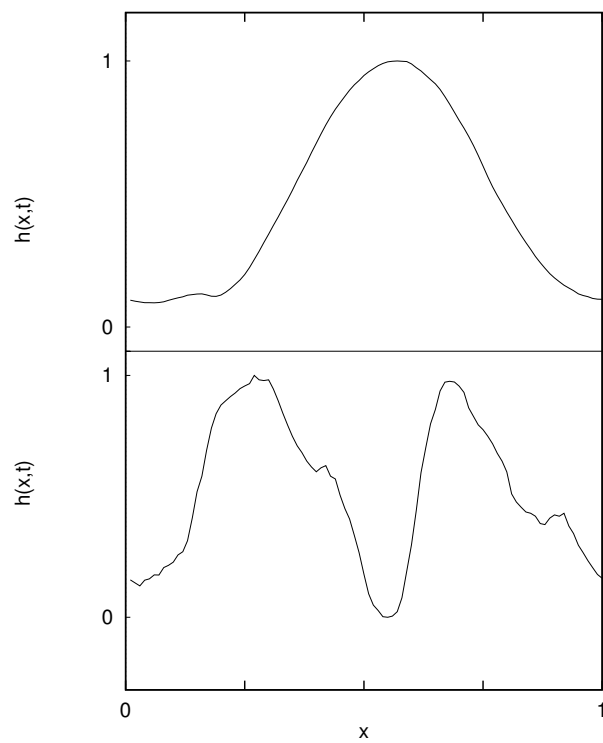
$$\begin{aligned} \text{cov}(x, y) &= \langle xy \rangle - \langle x \rangle \langle y \rangle \\ \text{var}(x) &= \langle x^2 \rangle - \langle x \rangle^2. \end{aligned}$$

Figure 4 shows the correlation coefficient as a function of distance  $R$ . For comparison with figures 2 and 3 we note the following: the range of  $x$  shown in figures 2 and 3 has been scaled to  $0 \leq x \leq 1$ . In figure 4,  $R$  is shown in the same units. We note that as long as  $R$  is small, the correlation function is nearly 1, showing that the height and densities at nearby points are strongly positively correlated. The correlation drops sharply to zero as  $R$  increases. The correlation virtually vanishes for  $R > 0.1$  units.

Figure 5 shows the height profile at long times  $t = 10^8$  for  $\nu = 0.01$  (top) and  $\nu = 10^{-6}$  (bottom). An investigation of this figure shows that a larger  $\nu$  has the overall effect of removing



**Figure 4.** The correlation function of the height and density profiles at large time  $t = 10^8$ , plotted against distance  $R$ ; both axes are logarithmic.  $\nu$  is taken to be 0.01.



**Figure 5.** A plot of  $h(x, t)$  against  $x$  for  $\nu = 10^{-6}$  (bottom) and  $\nu = 0.01$  (top).  $h(x, t)$  has been scaled to vary between 0 and 1 to facilitate a qualitative comparison.

local jaggedness; also, the larger the value of  $\nu$ , the earlier this effect appears. We explain this as follows: the term  $\rho|\nabla h|$  has a roughening effect, since the accretion it generates is *non-uniform*, depending, as it does, on the *local* density  $\rho(x, t)$ . On the other hand, the term  $\nu|\nabla h|$  generates a purely slope-dependent evaporation, which is asymptotically dominant and smoothing in its effect. Thus larger  $\nu$  should indeed generate a smoother profile in  $h$ , in accord with earlier work [2].

A more detailed description of the morphologies of the profiles can be obtained if we extract the critical roughening exponents  $\alpha$  and  $\beta$ . The critical exponents characterizing the temporal and spatial scaling behaviour of a rough surface can be obtained from the (connected) two-point correlation function:

$$S(x - x', t - t') = \langle h(x, t)h(x', t') \rangle - \langle h(x, t) \rangle \langle h(x', t') \rangle.$$

Figure 6 shows the behaviour of the correlation function  $S(R = x - x', t - t' = 0)$  for the height profile at three different time steps. As expected, the correlation length does indeed increase with time.

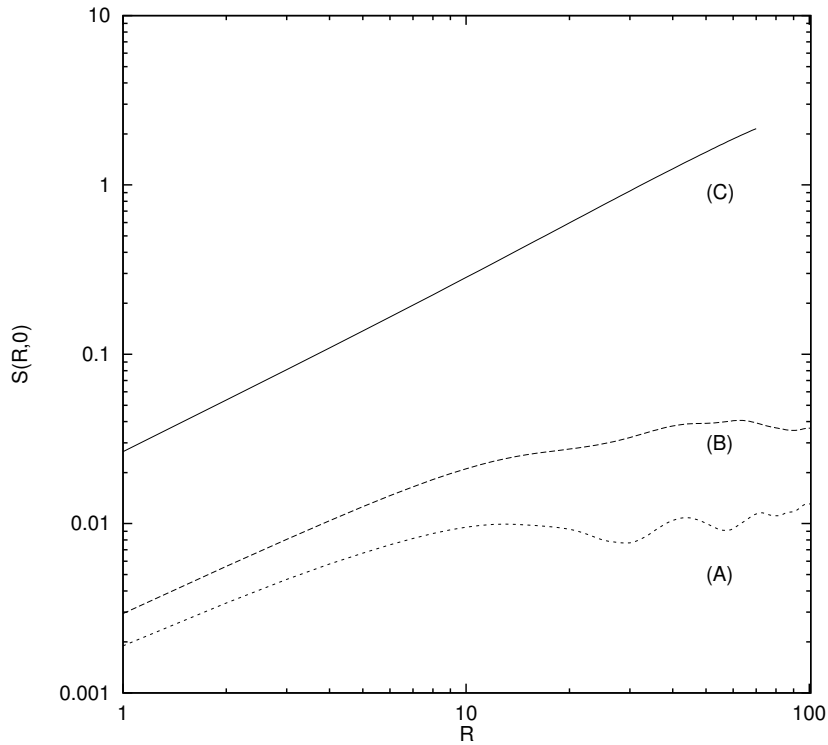


**Figure 6.** The correlation function  $S(R, 0)$  versus  $R$  for the height profile at three different times  $t = 10^4$  (curve A),  $10^5$  (curve B) and  $10^8$  (curve C) steps (bottom to top).

The single Fourier transforms of the correlation functions  $S(k, t - t' = 0)$  and  $S(x - x' = 0, \omega)$  define the two exponents  $\alpha$  and  $\beta$  via the relations

$$S(k, 0) \sim k^{-1-2\alpha}$$

$$S(0, \omega) \sim \omega^{-1-2\beta}.$$

A one-dimensional lattice was used in our simulations, with periodic boundary conditions.

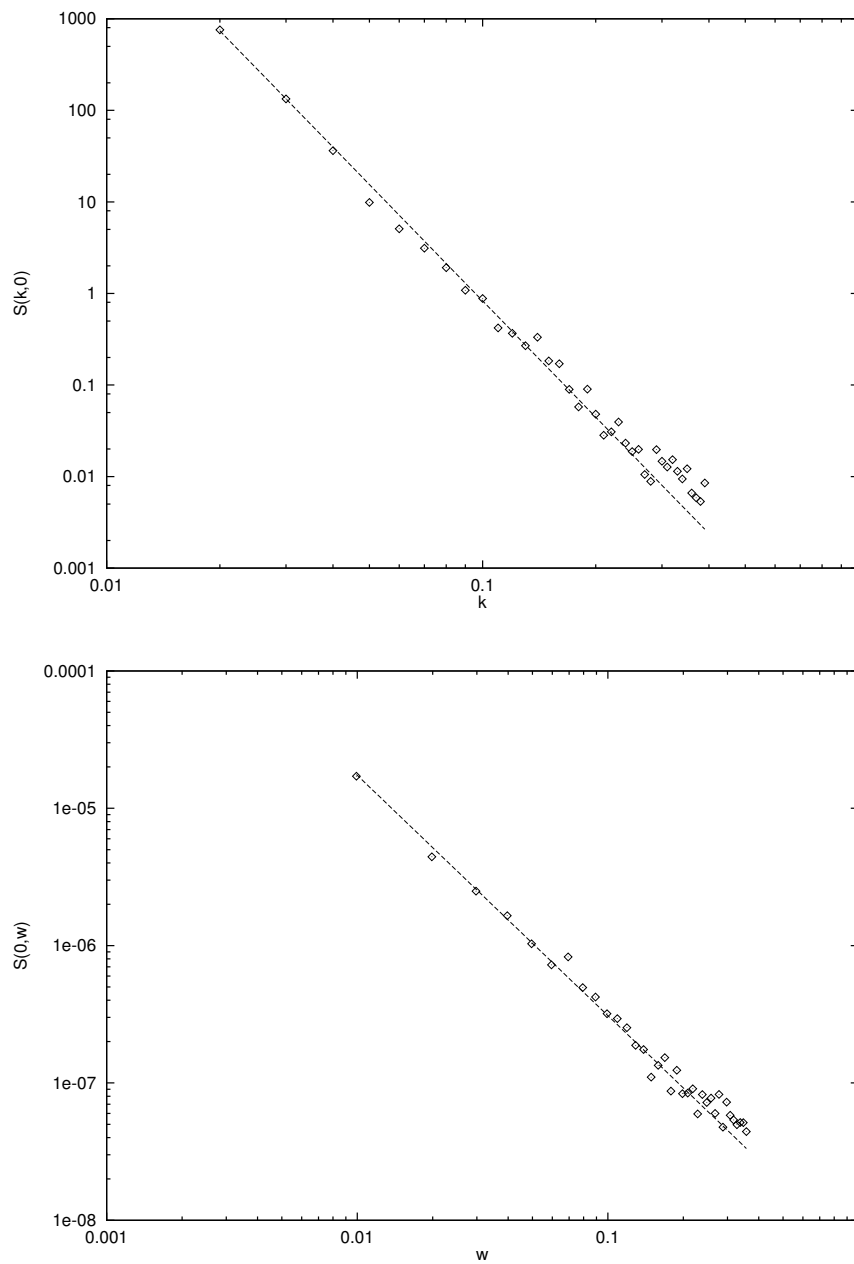


**Figure 7.** The Fourier transforms of the correlation functions  $S(k, 0)$  (top) and  $S(0, \omega)$  (bottom) for the height profile. Opposite: the Fourier transforms of the correlation functions  $S(k, 0)$  (top) and  $S(0, \omega)$  (bottom) for the density profile. The graphs are shown as log–log plots.

Finite-size checks were also carried out, in order to eliminate spurious effects arising from this in the determination of our critical exponents.

Figure 7 shows the results of our simulations via graphs of the dependence of  $S(k, 0)$  versus  $k$  and  $S(0, \omega)$  versus  $\omega$ , for each of the species  $h$  and  $\rho$ .

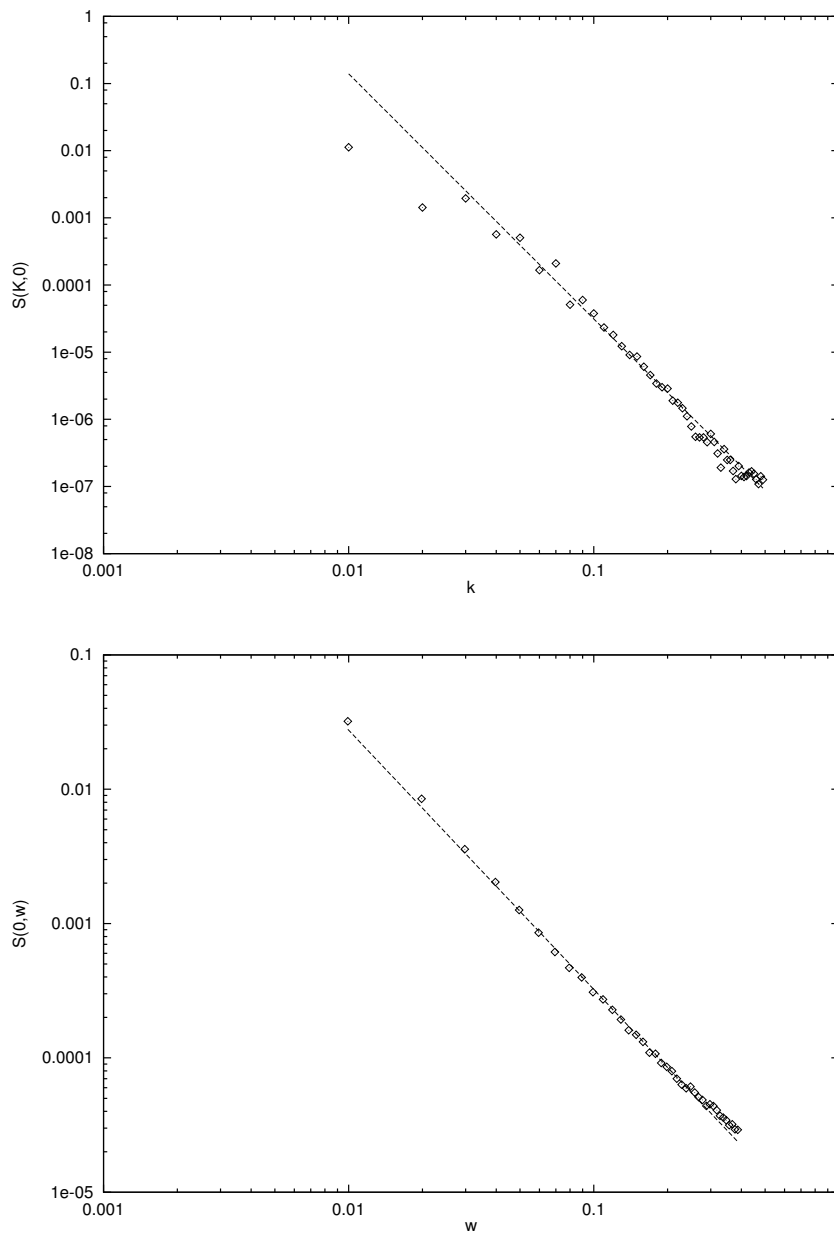


**Figure 7.** (Continued)

Our results are:

- (a)  $\alpha_h = 1.61 \pm 0.02$ ,  $\beta_h = 0.39 \pm 0.02$ ;
- (b)  $\alpha_\rho = 1.325 \pm 0.025$ ,  $\beta_\rho = 0.465 \pm 0.01$ .

The exponents for  $h$  indicate that the dynamical exponent is given by  $z_h \sim 4$ , consistent with most models for MBE growth [1], and indicating that the fourth-order term plays a

dominant role in the dynamics, as it should. However, the value of  $\alpha_h$  is greater, even given the error bars, than the pure WV value of 1.5; this suggests that the additional roughening is caused by the transfer term  $\mathcal{T}$ , which is therefore relevant in the renormalization-group sense.

The role of the transfer term  $\mathcal{T}$  is even more obvious in the critical exponents for  $\rho$ , where we get *super-roughening* in the mobile atoms. It is obvious that this can only arise from the transfer term, since without this one would have got purely diffusive exponents ( $\alpha_\rho = 0.5$ ,  $\beta_\rho = 0.25$ ) pertaining to the linear equation. The physics of this is as follows: the action of the  $\nabla^4 h$  term is to build up mounds and grooves on the bonded interface, as is well known. These then provide excellent sources of mobile atoms, because of the action of the  $\nu|\nabla h|$  term, in dislodging atoms from regions of high slope such as mounds and grooves. This *preferential generation* of mobile atoms in certain regions of the interface is what causes the excess roughening of the  $\rho$ -profile, as manifested by the large exponents for  $\alpha_\rho$  and  $\beta_\rho$  compared to a simple  $\nabla^2 \rho$  diffusive growth.

Before turning to the justification of our basic assumptions in the model, we have simulated profiles on a two-dimensional substrate with the same parameters as for our earlier model and  $\nu = 0.01$ . We have simulated the height profile both from the KPZ [9] model and our coupled equations. Figure 8 shows the KPZ profile in the top panel and the profile from our equations in the bottom panel. Both are for  $t = 10^{12}$ ; we note that the two profiles are very different in structure. Our profile is far smoother, in accord with the above discussion.

The reason that we have explicitly shown features evolving with time and at reasonably short timescales as well as local features (at short length scales) is that for most real deposited surfaces and overlayers, ‘universal’ behaviour is often irrelevant because asymptotic times and lengths are never reached in experiments.

We emphasize again that the values of the critical exponents above are those that would be obtained *in the limit of infinitely long times and in infinitely large systems*, which would not be realizable in typical experimental conditions. However, along the lines of earlier theoretical work (see, for example, Krug [1] or Das Sarma *et al* [7]) we nevertheless present our results as the bona fide conclusion of our investigations; and, importantly, *unlike* the case for most theoretical papers, we also add here possible avenues for experimental investigation. In recent work [10], we have linked the temporal and spatial exponents to *measured* quantities in the context of an experimental thin film; thus for example, an investigation separately of the diffuse and non-specular Bragg scattering intensities can be related to these exponents. We refer the interested reader to that paper.

#### 4. Electronic structure calculations

In this section, we perform electronic structure calculations in support of some of the terms in equation (2).

First, we examine the term  $\nabla^4 h$  and ask the question: is the assumption that the local chemical potential is proportional to the local curvature trivial? In his review article, Krug [1] implies that the reason for using local curvatures is simply a symmetry argument. However, he goes on to claim that a more realistic assumption would be to assert that the local chemical potential is proportional to the local bonding coordination. He obviously does not consider these two statements to be synonymous. It is important to realize that we are dealing here with metallic surfaces. Unlike in covalently bonded solids, where bonding can be considered to be two-by-two and mediated by the shared electron cloud, in a metal the bonding is via an itinerant electron cloud. It is not *a priori* clear that the chemical potential must depend on *local* properties. In other words, it is not trivial to assume that Heine’s ‘black-body theorem’ or equivalently the ‘short-sightedness’ paradigm of Kohn [12] holds for metallicly bonded

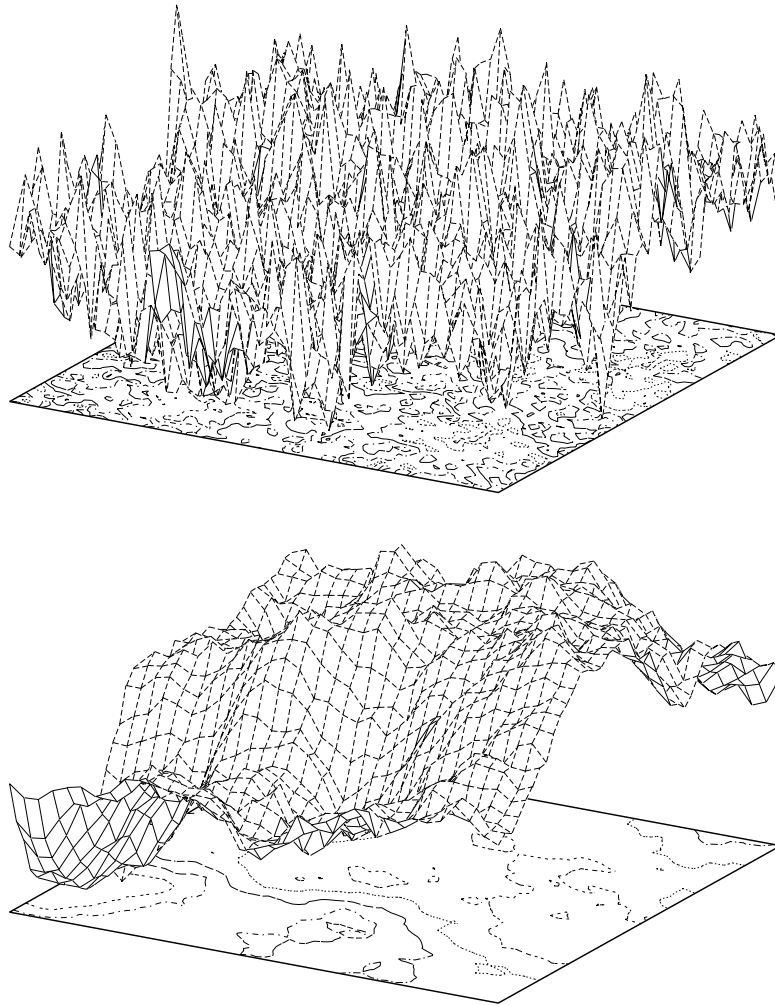


**Figure 8.** Height profiles for the KPZ model (top) and the coupled equations presented here (bottom).

surfaces. If the local chemical potential, i.e. the energy required to remove an atom from a given position on the surface, depends upon the topology over an extended region around it, then the assumption of proportionality to the local curvature may not be valid. In what follows, we attempt to justify this commonly made assumption by a detailed first-principles electronic structure calculation.

We take as our substrate surface a  $50 \times 50$  square lattice with the profile of heights properly reconfigured to get a three-dimensional body-centred cubic (bcc) overlayer. We use Hamiltonian parameters relevant to the growth of bcc Fe layers as overlayers on a face-centred cubic Ag(100) substrate. Since there is a close match between the bcc Fe lattice parameter and the edge-to-face atomic distance of Ag on the (100) surface, Fe grows easily and epitaxially on the Ag(100) surface without much strain. This system has been chosen to facilitate further work on magnetization at the interface, since interesting magnetic phenomena are known to

occur [13] when transition metal overlayers grow on noble-metal substrates.

Our procedure is as follows: we first produce rough profiles in  $h$  and  $\rho$  by numerically solving the coupled equations. The next step is to discretize the continuous variables  $h(x, t)$ . For a square lattice this discretization is straightforward. For a bcc lattice the heights can be thought of as produced by atoms vertically stacked in a edge–body–centre–edge sequence.

Most previous studies [13] on the energetics of surfaces have dealt with smooth surfaces, where use has been made of translational symmetry along the surface. These have involved surface Green functions  $G(k_{\parallel}, z)$  in which the Bloch theorem has been invoked parallel to the surface. In the perpendicular direction, calculations have been carried out in real space.

For a rough surface, however, lattice translation symmetry is lost in all three spatial directions: perpendicular to the substrate as well as on it. On such surfaces, therefore, the entire calculation should be carried out in real space. Although a coherent potential approximation [14] has been suggested in which one models rough surfaces as binary random alloys of the constituent atoms and *empty spheres*, it is doubtful whether homogeneous randomness (which is the basis of the coherent potential approximation) is suitable for describing the roughness involved. In a recent communication [15], we have modified the coherent potential approximation to include the effects of short-ranged ordering in surface layers. However, in all such alloy-analogy approaches, there is a basic underlying assumption of homogeneity which may not be appropriate for the systems considered here, since the formation of islands and clusters on epitaxially generated surfaces suggests that the randomness in these systems is highly inhomogeneous.

The recursion method of Haydock *et al* [16], however, does not require any assumption of homogeneity in the Hamiltonian. We suggest here the use of the recursion method. The feasible application of recursion requires a basis in which the Hamiltonian is sparse. The self-consistent tight-binding linearized muffin-tin orbitals (TB-LMTO) method based on the local spin-density approximation (LSDA) [17] provides exactly such a first-principles approach. The accuracy in energy obtained by the TB-LMTO method is of the order of 50 mRyd/atom. This is essential, since the chemical potentials are of the order of rydbergs, so our errors must be at least an order of magnitude less than those. In fact, in a recent communication Ghosh *et al* [18] have shown that the error in the recursion method is controllable, and have proposed an implementation of recursion where the error is always kept within a preassigned energy window.

The total energy per atom of the system is of the order of thousands of rydbergs, whereas the energy difference corresponding to the chemical potential (the energy difference between that of the system with a tracer atom bonded in a given configuration, and that with the tracer atom removed) is only a few rydbergs. The accurate estimation of such small differences of large numbers requires special numerical techniques. The orbital peeling method of Burke [19], which is closely related to the recursion method, provides us with just such a technique. This measures the energy barrier  $\mu$  that the tracer atom has to overcome by breaking its chemical bonding to neighbouring atoms before it diffuses.

The input potential parameters for the TB-LMTO Hamiltonian were first prepared by a supercell calculation. The unit cell was chosen to have three bcc Fe layers over nine Ag layers with three empty-sphere layers on top, in a tetragonal structure elongated in the (100) direction. In the supercell the overlayer is not rough. However, we use these Hamiltonian parameters as the *starting point* of our LSDA self-consistent recursion calculation for the rough overlayer covered with empty spheres carrying the spilled charge at the surface. The termination scheme of Luchini and Nex was used [20]. The charge density was generated from the local density of states and the LSDA potentials generated from them. This self-consistent potential included, in its Madelung part, the multipole contributions up to the dipole component of the surface

charge density as suggested by Kudrnovský *et al* [14].

The top panel in figure 9 shows the contour plot of this energy difference, delineated on the substrate. The tracer atom is placed on the top of the overlayer of height  $h(x, t)$  at various points  $x$  on the substrate. The bottom panel in figure 9 shows the corresponding contours of the local curvature at the tracer sites. The curvature is obtained from the nearest-neighbour configuration and is thus proportional to the coordination of the tracer atom. The figure clearly shows that  $\mu \propto \nabla^2 h$ , leading to a current  $j = \nabla(\nabla^2 h)$  which is the basis of the  $\nabla^4 h$  diffusive term in equation (2). The above justifies the assumption of Wolf and Villain [6, 11] that the local chemical potential is proportional to the local coordination for the metallic interfaces considered here. Our results also illustrate that the energetics in metallic interfaces have the ‘short-sightedness’ or local behaviour proposed by Heine [12].

We have also investigated the energetics resulting upon the variation of local slope  $|h(x+1) - h(x-1)|$ , in support of the  $v|\nabla h|$ , or *evaporation* term. The results (table 1)

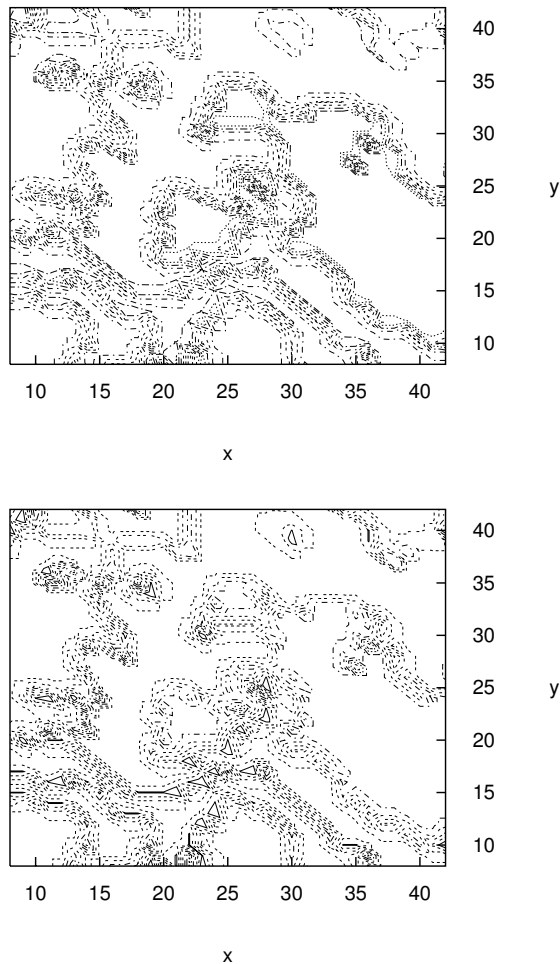


**Figure 9.** Top panel: a contour plot of the local chemical potential at different points on the overlayer on the planar substrate. Bottom panel: contour plots of the local curvature at the same points as in the top panel.

**Table 1.** The energy  $\Delta E$  required to remove a tracer atom from the interface as a function of the local slope magnitudes  $|\nabla h|$ .

$ \nabla h $	$\Delta E$ (Ryd)
1	1.27
2	1.19
4	1.16

show that as the magnitude of the local slope  $|\nabla h|$  around any given site increases, the energy  $\Delta E$  required to break the chemical bonds of a tracer atom decreases.

Each entry in the first column in table 1 is proportional to the magnitude of the slope at a site, and each entry in the second column gives the energy in rydbergs required to dislodge a tracer atom at that site. This verifies our contention that atoms sited in regions of high slope are relatively more unstable against the formation of the mobile species due to external thermal or mechanical disturbances, compared to those in regions of low slope. Lastly, we mention that a similar calculation in support of the *condensation* term  $\rho|\nabla h|$  is outside the scope of our present work, as it would require a dynamical analogue of the above energetics. Such calculations have been done in a different context using kinetic Monte Carlo [21] schemes. A full-fledged LSDA-based kinetic Monte Carlo calculation is in progress towards this end.

## References

- [1] Krug J 1997 *Adv. Phys.* **46** 1
- [2] Mehta A, Luck J M and Needs R J 1996 *Phys. Rev. E* **53** 92  
Biswas P, Majumdar A, Mehta A and Bhattacharjee J K 1998 *Phys. Rev. E* **58** 1266
- [3] Mehta A (ed) 1993 *Granular Matter: an Interdisciplinary Approach* (New York: Springer)
- [4] Car R and Parrinello M 1985 *Phys. Rev. Lett.* **55** 2471
- [5] Herring C 1951 *The Physics of Powder Metallurgy* ed W E Kingston (New York: McGraw-Hill)  
Mullins W W 1957 *J. Appl. Phys.* **28** 333  
Mullins W W 1959 *J. Appl. Phys.* **30** 77
- [6] Wolf D and Villain J 1990 *Europhys. Lett.* **13** 389
- [7] Das Sarma S, Lanczycki C J, Kotlyar R and Ghaisas S V 1996 *Phys. Rev. E* **53** 359 and references therein
- [8] Barabasi A 1992 *Phys. Rev. A* **46** R2977
- [9] Kardar M, Parisi G and Zhang Y C 1986 *Phys. Rev. Lett.* **56** 889
- [10] Mehta A and Cowley R A 1999 unpublished
- [11] Villain J 1991 *J. Physique* **1** 19
- [12] Heine V 1988 *Solid State Physics* vol 35 (New York: Academic) p 1
- [13] Blügel S 1995 *Lecture Notes in Surface Magnetism; Research Workshop in Condensed Matter Physics* (Trieste: ICTP)
- [14] Kudrnovský J, Wennien B, Drchal V and Weinberger P 1991 *Phys. Rev. B* **44** 4068  
Kudrnovský J, Turek I, Drchal V, Weinberger P, Christensen N E and Bose S K 1992 *Phys. Rev. B* **46** 4222
- [15] Sanyal B, Biswas P, Mookerjee A, Salunke H, Das G P and Bhattacharyya A K 1998 *J. Phys.: Condens. Matter* **10** 5767
- [16] Haydock R, Heine V and Kelly M J 1972 *J. Phys. C: Solid State Phys.* **5** 2845
- [17] Andersen O K and Jepsen O 1984 *Phys. Rev. Lett.* **53** 2571  
and see also  
Andersen O K, Jepsen O and Šob M 1987 *Electronic Band Structure and Its Applications* ed M Yussouff (Heidelberg: Springer) p 1
- [18] Ghosh S, Das N and Mookerjee A 1998 *J. Phys.: Condens. Matter* **9** 10701
- [19] Burke N R 1976 *Surf. Sci.* **58** 349
- [20] Luchini M U and Nex C M M 1987 *J. Phys. C: Solid State Phys.* **20** 3125
- [21] Ruggerone P, Ratsch C and Scheffler M 1997 *Growth of Ultrathin Epitaxial Layers (The Chemical Physics of Solid Surfaces vol 8)* ed D A King and D P Woodruff (Amsterdam: Elsevier Science)